Journal of Physiology (1990), **428**, *pp.* 441–466
With 15 figures
Printed in Great Britain

EXTRACELLULAR H^+ INACTIVATION OF Na^+–H^+ EXCHANGE IN THE SHEEP CARDIAC PURKINJE FIBRE

BY R. D. VAUGHAN-JONES AND MEI-LIN WU
From the University Laboratory of Physiology, Parks Road, Oxford OX1 3PT

(*Received 5 January 1990*)

SUMMARY

1. The inhibition of acid extrusion via Na^+–H^+ exchange caused by reducing pH_o (extracellular pH) was examined in the sheep cardiac Purkinje fibre. Intracellular pH (pH_i) and intracellular Na^+ activity (a^i_{Na}) were recorded using ion-selective microelectrodes. Acid extrusion via Na^+–H^+ exchange was estimated from the pH_i recovery rate (multiplied by intracellular buffering power, β) in response to an internal acid load induced by 20 mM-NH_4Cl removal (nominally CO_2–HCO_3-free media).

2. At a given pH_i, acid extrusion decreased sigmoidally with decreases of pH_o in the range 8·5 to 6·5 (50% inhibition of efflux occurred at a pH_o between 7·0 and 7·5). This inhibition was associated with a parallel decrease in Na^+ influx as evidenced from a decrease in the rise of a^i_{Na} measured during acid extrusion, suggesting inhibition of Na^+–H^+ exchange.

3. The background acid-loading rate (estimated by adding 1 mM-amiloride to inhibit Na^+–H^+ exchange and recording the initial rate of fall of pH_i) was found to be unaffected in the steady state by changes of pH_o. We therefore conclude that the slowing of pH_i recovery at low pH_o is due to direct inhibition of Na^+–H^+ exchange rather than to an increase of background acid loading.

4. Reducing pH_o (constant pH_i) inhibited acid efflux by producing a parallel shift of the efflux *versus* pH_i relationship to lower values of pH_i, consistent with a decrease in the apparent internal H^+ ion affinity (pK_i) of the system.

5. Raising pH_i (constant pH_o) also inhibited acid efflux, but this was associated with a rise in the pH_o required for 50% maximal inhibition of acid efflux (pK_o), consistent with an increase in apparent affinity for *external* H ions. Thus reduction of pH_o reduces pK_i (point 4) while reduction of pH_i reduces pK_o (point 5).

6. Inhibition by elevated H^+_o was not linearly related to the decrease in chemical driving force for Na^+–H^+ exchange, nor was it related to a reversal of the transmembrane H^+ gradient. We found that efflux still occurred when $pH_o < pH_i$.

7. Efflux was not a unique function of the transmembrane H^+ ratio (i.e. $pH_o - pH_i$). At appropriate values of pH_i and pH_o, acid efflux could be kept constant despite a four-fold change in the transmembrane H^+ ratio.

8. Inhibition by low pH_o was a saturating function of H^+_o ions with a Hill coefficient of 1·2. This is in contrast to the much steeper activation of efflux by

elevated H_i^+ ions, thus indicating asymmetry in H_i^+ activation and H_o^+ inhibition on either side of the membrane.

9. Possible models of H_o^+ inactivation of Na^+–H^+ exchange are discussed. It is also shown that the pH_i *vs.* pH_o relationship in the steady state will be a direct consequence of H_o^+ inactivation. Since this H_o^+ inactivation is $\sim 50\%$ complete at pH_o 7·4, changes of extracellular plasma pH will be important physiologically for modulating acid efflux from the heart.

INTRODUCTION

One major mechanism controlling pH_i in the mammalian heart is sarcolemmal Na^+–H^+ exchange (for review, see Vaughan-Jones, 1988*a*). A fall of pH_i activates acid extrusion via this system and a fall of pH_o inhibits it (Aronson, 1985). While intracellular activation by H^+ ions has been well characterized in many tissues, extracellular inactivation by H^+ ions has been examined less extensively. For cardiac muscle, only preliminary observations are available (Vanheel, de Hemptinne & Leusen, 1986; Weissberg, Little, Cragoe & Bobik, 1989). We have therefore characterized the inhibitory influence of extracellular acidosis upon Na^+–H^+ exchange in the sheep cardiac Purkinje fibre. Our experiments were done using ion-selective microelectrodes to record pH_i and a^i_{Na} (intracellular Na^+ activity) while experimentally manipulating the transmembrane H^+ ion gradient. We find that, in the physiological range, the dependence of Na^+–H^+ exchange upon pH_i and pH_o is asymmetric, the system being more sensitive to pH_i than pH_o. More importantly, we find that these pH sensitivities are not mutually exclusive. Alteration of pH_i affects the apparent affinity of the extracellular site for H^+ ions while alteration of pH_o affects apparent H^+ affinity at the intracellular site(s), a phenomenon reported previously for Na^+–H^+ exchange in rat brain synaptosomes (Jean, Frelin, Vigne, Barbry & Lazdunski, 1985). We test various hypotheses for the inhibitory effect of external acidosis and conclude that (i) it is not related in a simple linear manner to the decrease in thermodynamic driving force, (ii) it is not related to variation in passive H^+ influx via other (non-Na^+–H^+) pathways and (iii) it is not related to the size or direction of the transmembrane pH difference ($pH_o - pH_i$). Candidates remaining for the inhibitory mechanism are discussed.

The influence of pH_o upon Na^+–H^+ exchange will be important physiologically since H_o^+ inactivation is steepest in the range of pH 7·5–6·5, a range within which changes of extracellular pH occur quite commonly in the heart.

Preliminary reports of this work have been published (Wu & Vaughan-Jones, 1988; Vaughan-Jones & Wu, 1989; Vaughan-Jones, Wu & Bountra, 1989).

METHODS

General methods

General methods are similar to those described previously, e.g. Vaughan-Jones & Wu (1990). Briefly, thin (core diameter 100–200 μm) free-running Purkinje fibres were dissected from a fresh sheep heart, shortened to about 2 mm (by crushing the cut ends with fine forceps) and mounted in the perfusion chamber (volume $\sim 100\ \mu$l; perfused at $\sim 1{\cdot}0$ ml min^{-1}) at 37 °C.

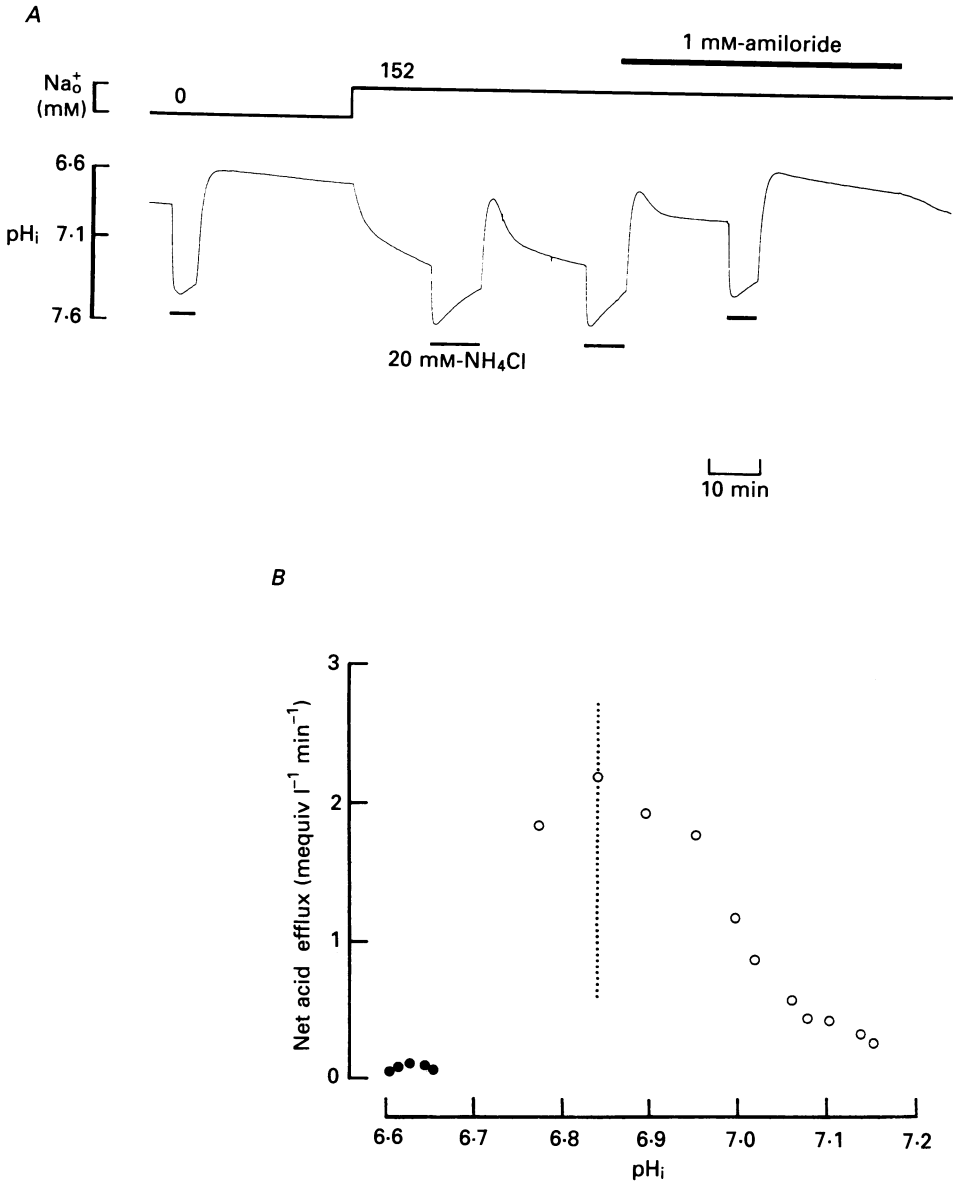

Fig. 1. pH_i recovery from an intracellular acid load is via Na^+–H^+ exchange. *A*, trace shows pH_i (recorded with a pH-selective microelectrode). Bars at bottom of figure denote period of superfusion of NH_4Cl (20 mM) while period in Na^+-free solution (*N*-methyl-D-glucamine substituted) and period of addition of 1 mM-amiloride are indicated at top of figure. *B*, graph showing acid efflux (as $\beta\, dpH_i/dt$; β estimated from eqn (1)), plotted *versus* pH_i under normal conditions (i.e. normal Tyrode solution with zero amiloride; ○) and in Na^+-free solution (●). Data from *A*. Point to left of dotted line in 'normal Tyrode' solution curve was measured < 2 min after NH_4Cl removal (see text for further details). Trace *A* has been modified from Fig. 2 of Vaughan-Jones & Wu (1990).

Solutions

Basic modified Tyrode solution contained (mM): NaCl, 140; KCl, 4·5; $CaCl_2$, 2·5; $MgCl_2$, 1·0; glucose, 11·0; HEPES buffer, 30; pH adjusted, as specified, to 7·4, 7·5 or 8·0 at 37 °C with 4 M-NaOH. For solutions of pH 6·5, 30 mM-PIPES (piperazine-*N*,*N*-bis-2-ethanesulphonic acid; pK_a 6·8) was substituted for HEPES in some experiments (e.g. Fig. 2), whereas in others, 30 mM-HEPES was adjusted to pH 6·5 (e.g. Fig. 6). There were no major differences in results analysed from either type of experiment. For solutions of pH 8·5, readjusted (NaOH) HEPES-buffered Tyrode solution was used *or* 30 mM-HEPPS (*N*-2-hydroxyethyl-piperazine-*N*-3-propane sulphonic acid; pK_a 8·0) was substituted for HEPES. Again, these differences in solution buffering caused no notable differences in the results.

Microelectrodes

Single-barrelled ion-selective microelectrodes were constructed and calibrated as described previously (Vaughan-Jones, 1988*b*; Vaughan-Jones & Wu, 1990) using liquid-sensor cocktails for H^+ ions (Fluka, code 95291) or Na^+ (Fluka cocktail code 227). Conventional microelectrodes used to record membrane potential were filled with 3 M-KCl and bevelled lightly before use (resistance 4–6 MΩ). Intracellular ion activity was recorded as the differential signal between an intracellular conventional microelectrode and an ion-selective microelectrode (ISM); electrode spacing 25–100 μm. For multiple intracellular ion recordings (e.g. Fig. 6) the ISM signals were referred to a common membrane potential microelectrode. For recordings of extracellular surface pH (pH_s), the pH electrode signal was referred to a blunt 3 M-KCl-filled reference electrode placed in the bulk solution.

pH_i recovery represents Na^+–H^+ exchange

In this paper, Na^+–H^+ exchange is examined by recording the rate of pH_i recovery following an intracellular acid load. The load was induced by external addition and subsequent removal of 10–20 mM of the weak base, NH_4Cl (ammonium pre-pulse technique, see Roos & Boron, 1981). Figure 1*A* shows that, in HEPES-buffered Tyrode solution nominally free of CO_2–HCO_3, normal recovery of pH_i from the acid load occurs within about 20 min and is mediated almost exclusively via Na^+–H^+ exchange. In the absence of Na_o^+ (substituted by *N*-methyl-D-glucamine), pH_i recovery is slowed greatly and this inhibition is similar to that observed in the presence of 152 mM-Na_o^+ plus 1 mM-amiloride (an inhibitor of Na^+–H^+ exchange). Net acid efflux estimated from the pH_i recovery rate in normal Tyrode solution is plotted *versus* pH_i in Fig. 1*B* (○). Acid efflux (J_e) has been estimated as $\beta\, dpH_i/dt$ where β = intrinsic non-CO_2 buffering power. dpH_i/dt was determined from original pen recordings using measurements of the change in pH_i during set time intervals (usually 70–120 s). Since β varies inversely with pH_i, it was estimated using the empirical equation determined recently for the Purkinje fibre by Vaughan-Jones & Wu (1990):

$$\beta = -19{\cdot}6\ pH_i + 160. \quad (1)$$

Apparent acid efflux has also been estimated for the slow pH_i recovery observed in Na^+-free solution (●). It is clear from Fig. 1*B* that virtually all acid efflux can be attributed to Na^+–H^+ exchange.

The problem of slow acid loading following an ammonium pre-pulse

Bountra, Powell & Vaughan-Jones (1990) have shown recently that in isolated guinea-pig papillary muscle, the intracellular acid loading produced by the ammonium pre-pulse technique takes several minutes. As a consequence, pH_i recovery from the acidosis may be severely slowed because of continued slow acid loading. Figure 1*A* (modified from Fig. 2 of Vaughan-Jones & Wu, 1990) indicates that this is not a major problem in the Purkinje fibres selected for the present study. The true acid-loading time can be estimated from the loading time seen in Na^+-free solution (i.e. in the near absence of acid extrusion). In Fig. 1*A*, this is about 2 min; measurements of normal acid extrusion made 2 min or more after NH_4Cl removal are indicated to the right of the vertical dotted line in Fig. 1*B* (○). These measurements should therefore be uncontaminated by residual acid loading. The apparent saturation of efflux at low pH_i seen to the left of the dotted line is likely to be artifactual since efflux measurements in this region are made < 2 min after NH_4Cl removal so that residual acid loading will still be significant. In a total of seven fibres, acid loading (20 mM, ammonium pre-pulse) in Na^+-free solution was 50 % complete after 1·06 ± 0·12 min. For comparison,

in thirteen fibres, pH_i recovery in normal Tyrode solution was 50% complete within 8·5 ± 1·07 min. When analysing pH_i recoveries in this paper (e.g. Fig. 8) we have therefore taken data > 4 min after NH_4Cl removal. As a rule of thumb, if measurements of acid efflux in the Purkinje fibre are made on the near-linear phase of the efflux *versus* pH_i curve (see Fig. 1*B*), then they should be uncontaminated.

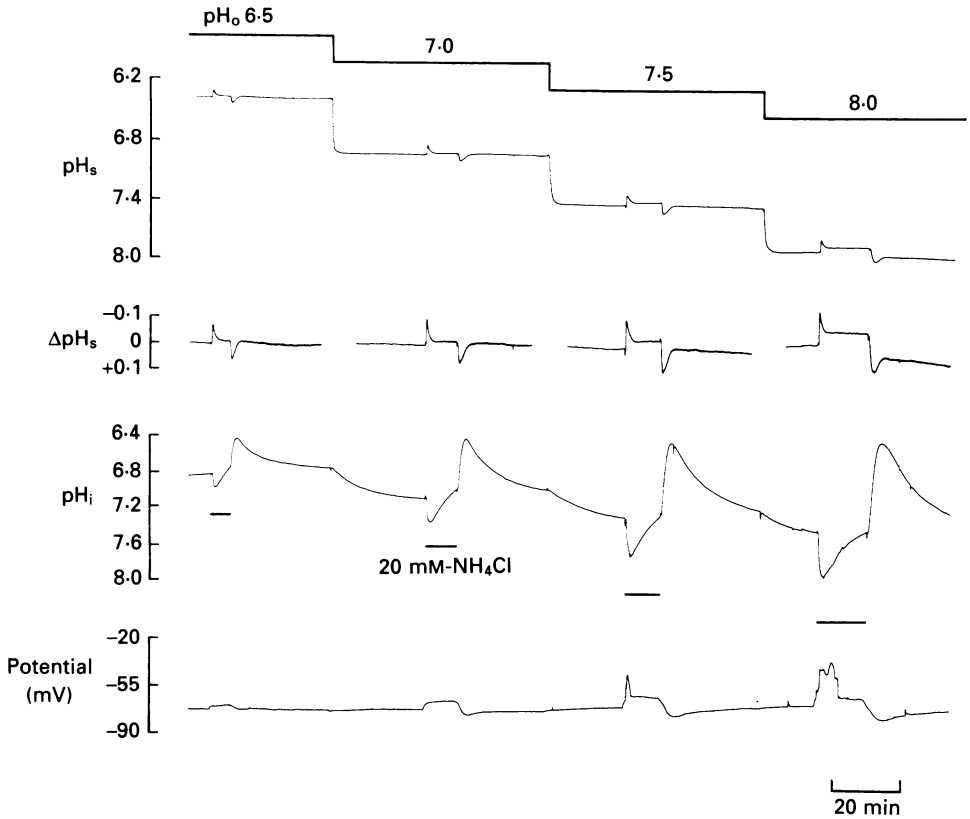

Fig. 2. pH_i recovery is influenced by pH_o. Traces show (top to bottom) (i) extracellular, surface pH (pH_s) recorded by positioning a blunt pH electrode close to the Purkinje fibre surface; (ii) a higher gain recording of pH_s; here, for convenience, the large DC changes of pH_s upon changing pH_o (indicated at top of figure) have been removed; (iii) pH_i; (iv) membrane potential. An internal acid load was induced by adding and removing 20 mM-NH_4Cl (indicated under pH_i trace). Solution contained 30 mM-PIPES (pH_o 6·5); 30 mM-HEPES (pH_o 7·0, 7·5); 30 mM-HEPPS (pH_o 8·0).

Changes of surface pH

One further source of error may be caused by changes in pH_s (surface pH; Vanheel *et al.* 1986). Addition and removal of NH_4Cl produces transient changes in pH_s as shown in Fig. 2. Note that during intracellular acid loading (NH_4Cl removal), pH_s becomes transiently alkaline. This is caused by NH_3 efflux from the cell and subsequent hydration to form NH_4^+ ions in the extracellular space: thus pH_s rises. Once all NH_3 has departed, pH_s should return to normal or may even become acidic owing to acid efflux on Na^+–H^+ exchange (Vanheel *et al.* 1986). The important point to note in Fig. 2 is that, after the initial pH_s transient following NH_4Cl removal, pH_s is reasonably constant throughout each pH_i recovery and pH_s is close to pH in the bulk solution. Thus the pH_o dependence of acid extrusion described in this paper will not be distorted by unwanted changes in pH_s.

Statistics

These are expressed as means ± standard error of the mean (S.E.M.).

RESULTS

Effect of changing pH_o upon pH_i recovery

Figure 2 shows an experiment where addition and removal of 20 mM-NH_4Cl was performed at four values of pH_o ranging from 6·5 to 8·0. By varying the time of exposure to NH_4Cl, the same peak intracellular acidosis of ~ 6·4 was achieved in each case. The exposure time was judged by observing pH_i: the higher the pH_o, then the higher the pH_i value at which one had to remove external NH_4Cl. Intracellular pH recovered from each acid load. Note, however, that with higher values of extracellular pH, the recovery proceeded to a more alkaline pH_i. Figure 3*A* shows that the time course of each pH_i recovery can be approximated to an exponential process whose half-time ($t_{0·5}$) is essentially independent of pH_o (Fig. 3*B*). The same observation was made in four other fibres. Similar parallel pH_i recoveries with time have been observed recently upon varying pH_o in cultured superior cervical ganglion cells (Tolkovsky & Richards, 1987). Since the extent of pH_i recovery (ΔpH_i) is greater at more alkaline pH_o and since $t_{0·5}$ is constant, we conclude that recovery rate increases with increasing pH_o (pH_i recovery rate = ΔpH_i ($t_{0·5}$/0·693)). This is consistent with previous observations on Na^+–H^+ exchange in a variety of tissues (Aronson, 1985) including cardiac muscle (Vanheel *et al.* 1986; Weissberg *et al.* 1989). Before the phenomenon can be ascribed to a direct effect of pH_o on the exchanger, one must inquire if changing pH_o alters pH_i via mechanisms other than Na^+–H^+ exchange. For example, reducing pH_o could conceivably increase a passive, acidifying leak into the cell which would slow pH_i recovery thus giving the illusion of inhibition.

Influence of pH_o upon the background rate of acid loading

Figure 4*A* shows that application of a high dose (1 mM) of amiloride results in a reversible acidification. Assuming that this is due to inhibition of Na^+–H^+ exchange (e.g. Kaila & Vaughan-Jones, 1987), then the initial rate of acidification in amiloride must equal the background rate of acid loading normally balanced by acid efflux on the exchanger. Figure 4*A* shows that applying amiloride produces similar rates of loading when pH_o is 8·0, 7·4 and 6·5. Table 1 shows data averaged from several fibres. The mean initial acid-loading rate in amiloride is not significantly different at three values of pH_o indicating that, in the steady state, background loading is independent of pH_o. The slowing of pH_i recovery at low pH_o (Fig. 2) is therefore not due to an increased acid loading of the cell.

The background loading could be caused either by passive acid influx or by generation *de novo* of acid within the cell. Data shown in Fig. 4*B* suggest that acid generation is the explanation. Prolonged application (> 40 min) of 10 mM-2-deoxyglucose (DOG) (in glucose-free Tyrode solution) in order to inhibit glycolysis (Allen, Morris, Orchard & Pirolo, 1985; Bountra, Kaila & Vaughan-Jones, 1988) produced a transient alkalosis followed by a sustained acidosis of 0·25 pH units (cf. Bountra *et al.* 1988). The rate of acid loading produced by adding amiloride was then greatly reduced, e.g. in Fig. 4*A*, acid loading in amiloride was 0·014 pH units min^{-1}, measured at a pH_i 6·91 and pH_o 6·5; in the presence of deoxyglucose (Fig. 4*B*) acid loading in amiloride was reduced by 75% to 0·003 pH units min^{-1} (measured at 6·86 pH_i and 6·5 pH_o). A similar result was obtained (not shown) when 0·5 mM-

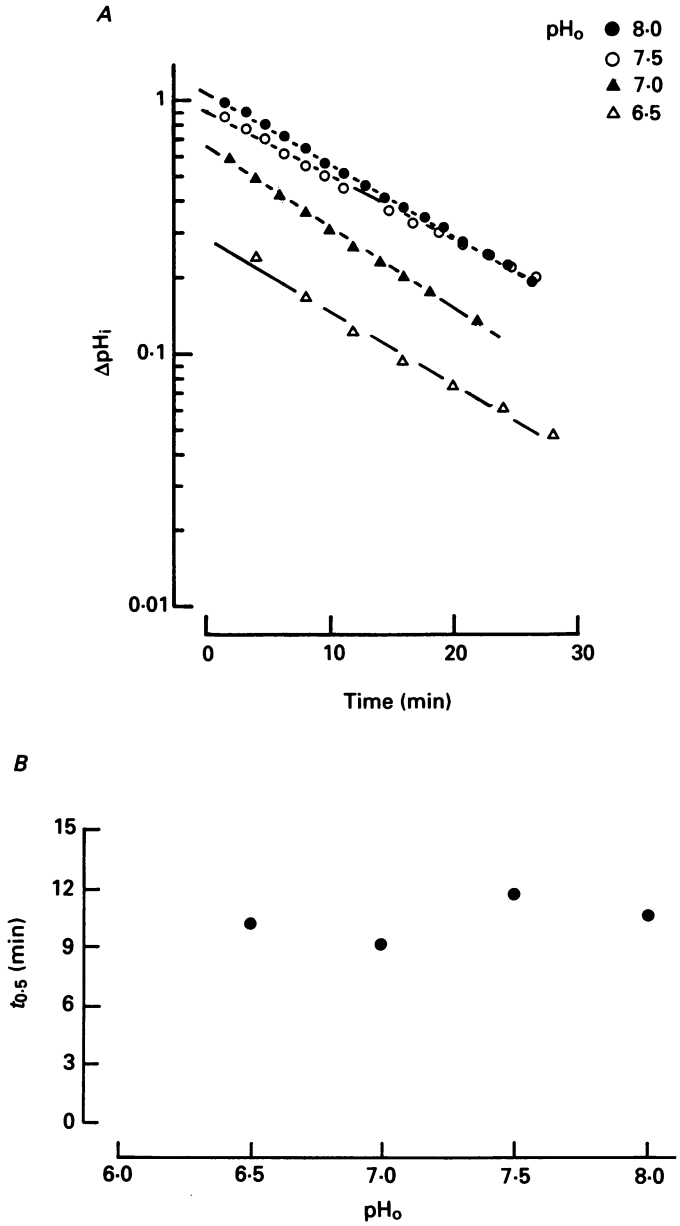

Fig. 3. pH_i recovery is roughly exponential with a half-time that is independent of pH_o. *A*, the time course of the four pH_i recoveries shown in Fig. 2 is replotted on semilogarithmic axes (ordinate shows log ΔpH_i, where ΔpH_i is the difference between pH_i at a given time during the recovery and the final pH_i value at the end of the recovery). *B*, the half-time for pH_i recovery ($t_{0.5}$) is plotted *versus* pH_o. Data from *A*.

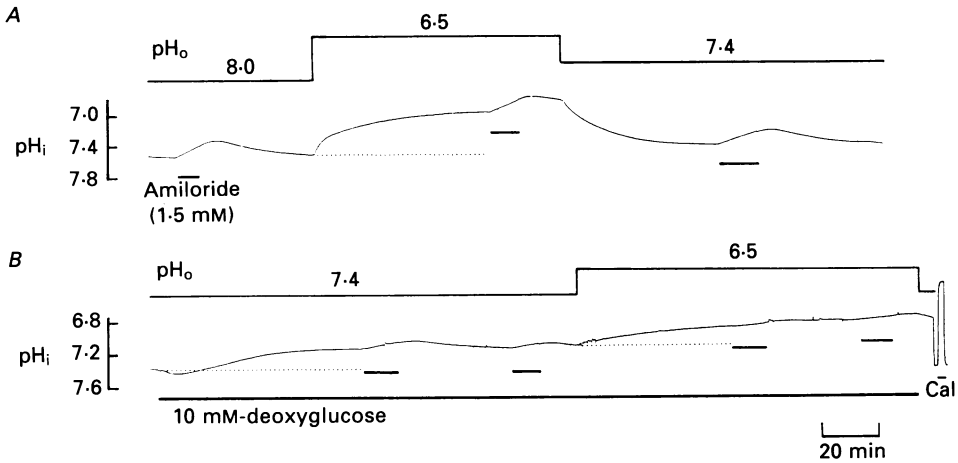

Fig. 4. Rate of background acid loading is independent of pH_o. *A*, experimental protocol. Background loading was estimated by adding amiloride (1·5 mM) to inhibit acid extrusion (bars under pH_i trace). Changes of pH_o are indicated at top of figure. Note that pH_i was allowed to stabilize in each new pH_o before amiloride was added. *B*, deoxyglucose (DOG, 10 mM in glucose-free solution) reduces steady-state background loading (revealed by adding 1·5 mM-amiloride). Extracellular calibration of pH electrode shown at end of figure (Cal). *B* is continuation of experiment shown in *A*.

TABLE 1. Steady-state background acid loading at various pH_o, determined by adding 1 mM-amiloride

pH_o	Mean pH_i	Background acid loading rate (mequiv l^{-1} min^{-1})
8·0	7·38 ± 0·01	0·10 ± 0·01 (n = 4)
7·4	7·17 ± 0·04	0·10 ± 0·02 (n = 5)
6·75	6·95 ± 0·04	0·09 ± 0·01 (n = 4)

Loading $= -\beta\, dpH/dt$. Values represented as means ± S.E.M.

iodoacetate rather than deoxyglucose was used to inhibit glycolysis. Most background acid loading therefore appears to be metabolic which may help explain its insensitivity to changes of pH_o.

Upon reducing pH_o, pH_i falls relatively rapidly (Fig. 4*A*) and then stabilizes within 20–30 min. The nature of this initial fall of pH_i is unclear. It cannot be caused by thermodynamic reversal of Na^+–H^+ exchange since pH_o is not sufficiently low (a $pH_o < 6{\cdot}30$ would be required, assuming $a^i_{Na} = 7{\cdot}5$ mM). Chloride–bicarbonate exchange is unlikely to be involved since all solutions were nominally free of CO_2–HCO_3. The fall of pH_i with pH_o persists in the presence of DOG (although the rate of fall may possibly be reduced, Fig. 4*B*) and so cannot be attributed entirely to anaerobic metabolism. The initial rate of internal acid loading is also much more rapid than that measured by applying amiloride in the steady state (Fig. 4*A*). These observations would be consistent with an increased, background H^+ influx at low pH_o. The increase, however, would have to be *transient* since, in the steady state, the background acid loading is unchanged, as judged from the constant loading rate in amiloride. Thus, although there is some evidence for a transient pH_o-sensitive acid loading in the Purkinje fibre, this will not affect our analysis of pH_i recovery since, upon changing pH_o, we always permitted pH_i to relax to a steady state before performing an ammonium rebound (see Figs 2 and 6).

In the experiment of Fig. 5*A* we investigate whether, at constant pH_o, background acid generation varies with *intracellular* pH. Removal of Na_o^+ (thus inhibiting Na^+–H^+ exchange) initially produced a small transient intracellular acidosis followed by a slower, continuous decline of pH_i comparable to that seen with amiloride. This

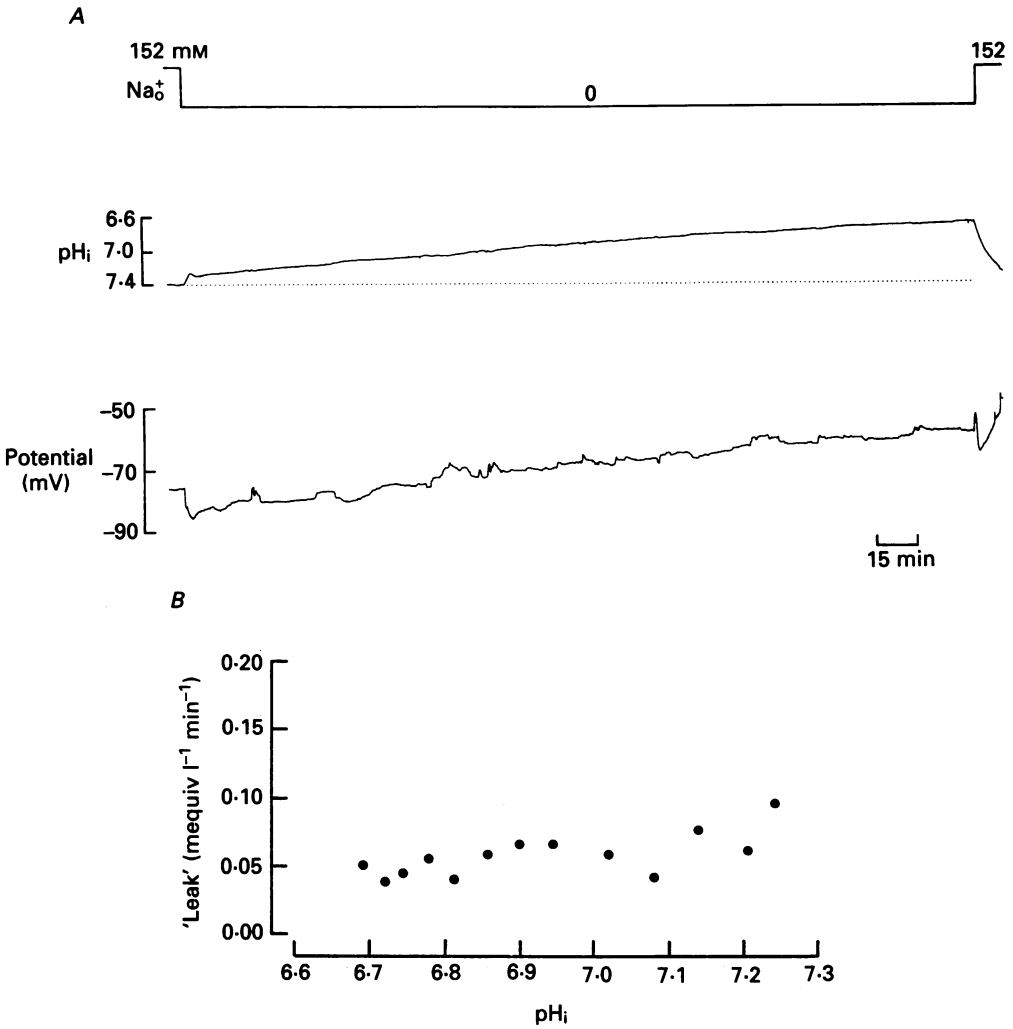

Fig. 5. Revealing the background acid-loading rate by inhibiting acid extrusion in Na^+-free solution. *A*, experimental protocol. Na_o^+ replaced by N-methyl-D-glucamine (indicated at top). Traces show (upper) pH_i and (lower) membrane potential. *B*, acid loading in Na^+-free solution (labelled 'leak' and calculated as $-\beta\, dpH_i/dt$) is plotted *versus* pH_i; data from *A*.

is therefore likely to reflect background loading. Possible reversal of Na^+–H^+ exchange (or Na^+–Ca^{2+} exchange) in Na^+-free solution will not be a contributing factor after 10 min since Na_i^+ falls within a few minutes to $< 0{\cdot}5$ mM (Ellis, 1977). Figure 5*B* plots the rate of acid loading (calculated as $-\beta\, dpH_i/dt$) as a function of pH_i during Na^+-free treatment. Despite some scatter, the background loading rate

appears to be reasonably constant ($\sim 0{\cdot}05$ mM l^{-1}, similar to the loading rates listed in Table 1) in the pH_i range from 6·7 to 7·2 (there may be a trend towards slightly lower loading rates at low pH_i). Thus, during pH_i recovery from an acid load, a constant term (z) should be added to estimates of acid efflux (J_e),

$$J_e = \beta \, dpH_i/dt + z, \tag{2}$$

(where z is, on average, 0·1 mM l^{-1}; see Table 1) in order to allow for efflux which balances background metabolic loading. This addition has been done in all subsequent measurements of J_e presented in this paper. In some cases z was determined directly by amiloride addition in the same experiment. In the cases where this was not done, a value for z of 0·1 mM l^{-1} was assumed. Note that this correction value is small compared with the total magnitude of J_e estimated during pH_i-recovery from an acid load (Figs 8, 9, 12 and 13).

Raising pH_o directly stimulates Na^+–H^+ exchange

Figure 6 shows an experiment where a^i_{Na} was recorded as well as pH_i. This experiment provides firm evidence for stimulation of Na^+–H^+ exchange since the acceleration in pH_i recovery from an internal acid load at high pH_o was accompanied by an increased overshoot of a^i_{Na}. The rise of a^i_{Na} is caused by Na^+ influx on Na^+–H^+ exchange (Deitmer & Ellis, 1980; Piwnica-Worms, Jacob, Horres & Lieberman, 1985; Kaila & Vaughan-Jones, 1987) and so the initial rate of rise of a^i_{Na} should provide an estimate of this influx. In Fig. 6, it is apparent that (for a constant internal acid load) the rise of a^i_{Na} accelerated when pH_o was made more alkaline. This effect has been plotted in Fig. 7 which shows that Na^+ influx increases sigmoidally with pH_o, displaying evidence of saturation at pH_o 8·5. Activation is 50% complete at pH_o 7·05. These data, which are independent of pH_i measurement, provide final proof that Na^+–H^+ exchange is stimulated by a rise of pH_o.

Effect of pH_o upon the pH_i dependence of acid extrusion

Figure 8 presents data obtained from an experiment similar to that shown in Figs 2 and 6. The data are plotted in the form of a series of activation curves for acid efflux as a function of pH_i, measured at various values of pH_o. Acid efflux was calculated using eqn (2); the appropriate value for β (intracellular buffering power) in this equation was calculated from eqn (1). The relationships are not linear since there is clear evidence of a 'foot' to the activations observed at the higher values of pH_i. Nevertheless, over much of the range of pH_i, the data form a series of roughly parallel lines. This is to be expected since Figs 2 and 3 have shown that pH_i recovery at various pH_o can be approximated to an exponential process possessing a common half-time. Figure 8 indicates that reduction of pH_o inhibits acid efflux by shifting the pH_i dependence of extrusion to the left along the abscissa (to lower values of pH_i). For a fall of pH_o from 8·0 to 7·0 (1·0 pH units), there is a leftward shift of about 0·3 pH units with virtually no change in slope. A similar result was obtained in four other fibres. It is notable that, in all fibres tested, for successive 0·5 pH unit decreases in pH_o from 8·5 to 6·5 the leftward shift of the pH_i curve became successively larger. For example, in Fig. 8, the shift was greatest for the pH_o decrease from 7·5 to 7·0. We return to this observation in the next section.

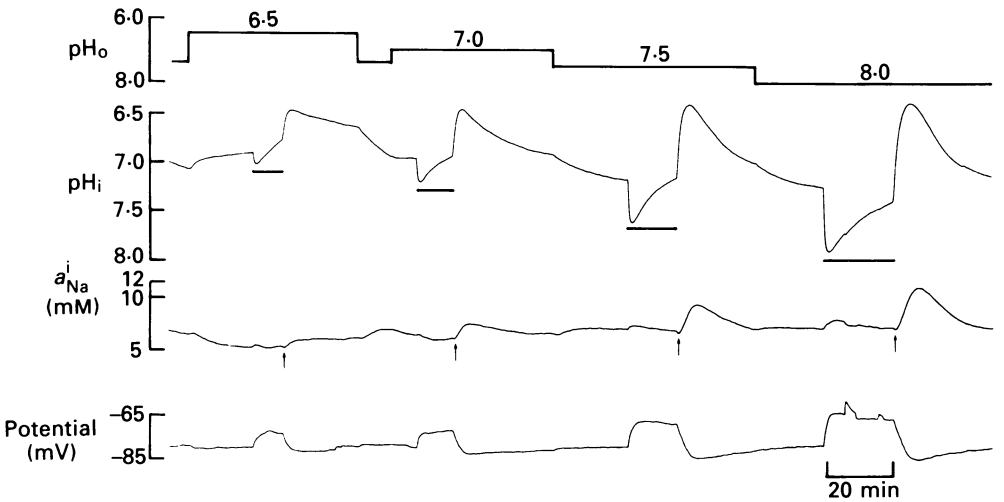

Fig. 6. Acceleration of pH_i recovery upon raising pH_o is accompanied by acceleration in the rise of a^i_{Na}. Changes of pH_o indicated at top of figure. Traces show pH_i (upper), a^i_{Na} (middle) and membrane potential (lower). Short bars under pH_i trace indicate periods of application of NH_4Cl (20 mM). Vertical arrows under a^i_{Na} trace indicate the rise of a^i_{Na} caused by reducing pH_i at various values of pH_o. Solutions buffered with 20 mM-HEPES.

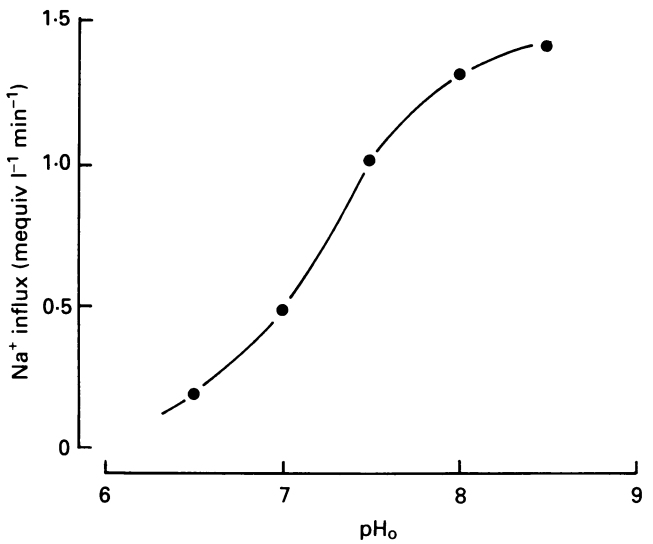

Fig. 7. At constant pH_i, Na^+ influx (via Na^+–H^+ exchange) increases with pH_o. Data from Fig. 6, Na^+ influx expressed as $0{\cdot}75^{-1}$ (da^i_{Na}/dt) where da^i_{Na}/dt was measured at a pH_i of 6·65 during the intracellular acid loads induced by removing NH_4Cl (20 mM). The data are converted from activity to concentration changes per unit time by dividing by 0·75 (assumed intracellular Na^+ activity coefficient).

The leftward shift suggests a decrease in the apparent intracellular H^+ ion affinity (pK_i) of the exchanger in response to a decrease in pH_o (i.e. a decrease in the pH_i required for 50% activation of efflux.). Unfortunately, we cannot directly measure pK_i since we have no estimate of the maximum extrusion rate at low pH_i ($V_{max,i}$). If

we assume that $V_{max,i}$ is unaffected by changes in pH_o, then the leftward shift (Fig. 8) suggests that pK_i decreases by about 0·3 pH units for a 1·0 decrease in pH_o. A similar result was obtained in four other fibres. Clearly, if $V_{max,i}$ is also reduced by lowering pH_o, then the above fall in pK_i will have been overestimated. We return to this point in the Discussion.

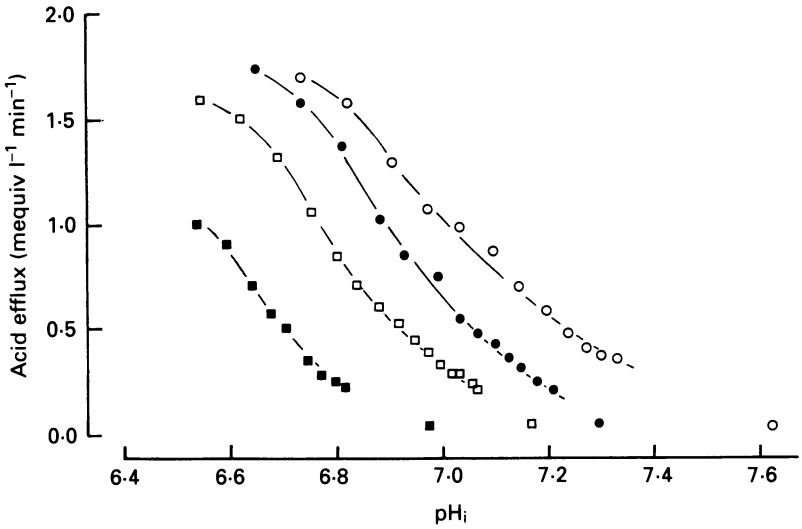

Fig. 8. Influence of pH_o upon pH_i dependence of acid extrusion. Acid efflux (β dpH_i/dt) during pH_i recovery from an ammonium pre-pulse is plotted *versus* pH_i under conditions where pH_o was 8·5 (○), 8·0 (●), 7·5 (□) and 7·0 (■). Data taken from an experiment similar to that shown in Figs 2 and 6. The four individual points shown at the base of the four curves denote pH_i achieved in the steady state (acid efflux in the steady state was assumed to equal the mean value of 0·1 mequiv l^{-1} min^{-1} quoted for background acid loading in Table 1).

The effect of pH_i upon the pH_o dependence of acid extrusion

The effect of varying pH_o upon acid extrusion (at constant pH_i) has already been estimated (Fig. 7) from changes in the counter-influx of Na^+. A similar sigmoidal relationship is evident if one examines the pH_o sensitivity of pH_i recovery. Figure 9 shows a plot of acid efflux as a function of pH_o, data being taken from Fig. 6. We have estimated acid efflux at four different levels of pH_i. In all cases acid efflux increases with pH_o in the range from 6·5 to 8·5 with signs of saturation as pH_o approaches 8·5. This was also the case in four other fibres.

Saturation is consistent with the observation (see previous section) that the parallel shift in the pH_i curve with change of pH_o is smallest at high values of pH_o. Not also that the acid efflux curve measured at pH_i 6·65 (Fig. 9) matches closely the Na^+ influx curve estimated (Fig. 7) in the same experiment (at $pH_i \sim 6{\cdot}7$) thus demonstrating that the exchange fluxes derived from pH_i and a^i_{Na} measurements are in good stoichiometric agreement.

Figure 9 indicates that reducing pH_i influences the size and shape of the relationship between acid efflux and pH_o. Two important effects are evident: (i) there

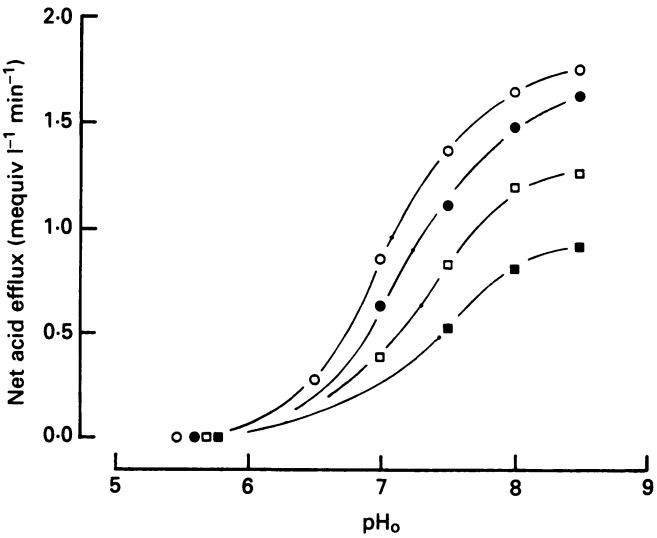

Fig. 9. Influence of pH_i upon the pH_o dependence of acid extrusion. Data taken from experiment shown in Fig. 6. For a constant value of pH_i (6·65, ○; 6·75, ●; 6·85, □; 6·95, ■) acid efflux has been estimated (eqn (2)) at various values of pH_o. Curves drawn by eye. The dots on each curve indicate pH_o at 50% maximal efflux (i.e. pK_o). Note that, at lower values of pH_i, pK_o is also lower. The points at the base of the four curves denote zero efflux. These indicate pH_o at which Na^+–H^+ exchange is at thermodynamic equilibrium. These zero points were calculated using the equation:

$$pH_o(\text{equilibrium}) = pH_i - \log_{10}\frac{Na_o^+}{Na_i^+},$$

where $Na_o^+ = 148$.

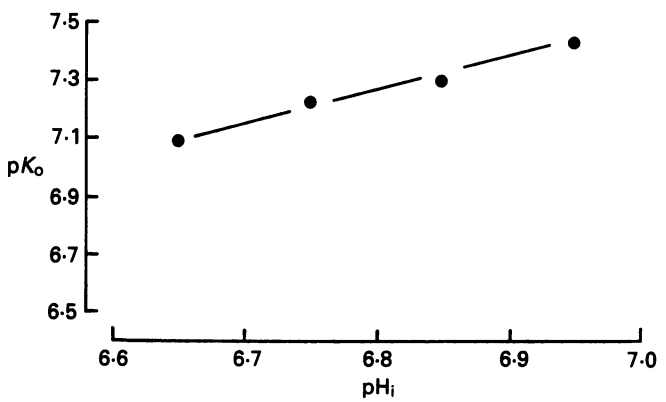

Fig. 10. Influence upon pK_o (apparent external H^+ ion affinity) of a change in pH_i. Data taken from Fig. 9. Line fitted by least-squares linear regression.

is an *increase* in $V_{max,o}$ (maximal rate at high pH_o) and (ii) there is a reduction in pK_o ($pK_o = pH_o$ at 50% maximal acid efflux). The increase in $V_{max,o}$ was expected since, even at alkaline levels of pH_o (8·0–8·5) the exchanger remained non-saturated with respect to pH_i (see Fig. 8). The decrease in pK_o, however, was not anticipated

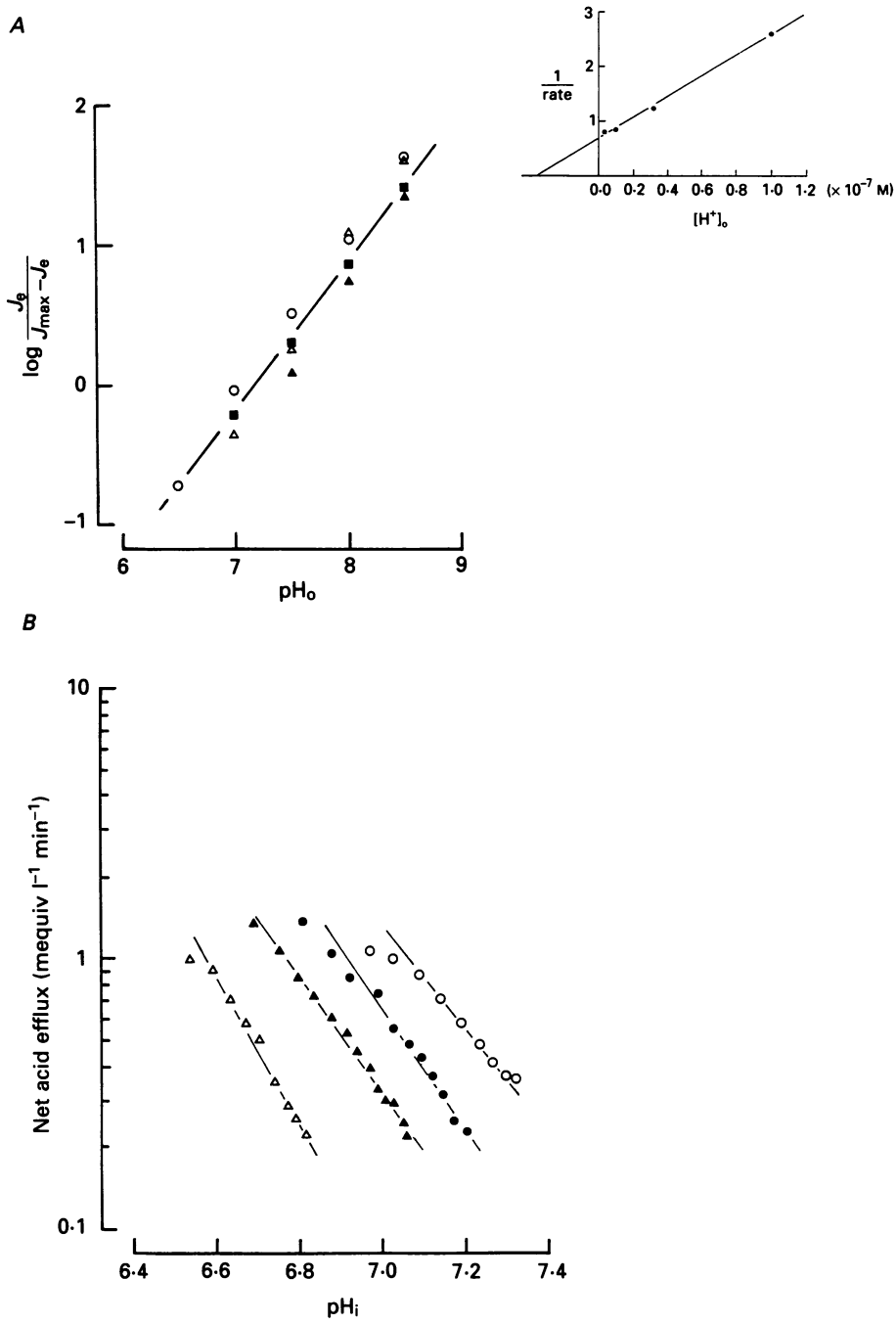

Fig. 11. Comparison of pH_i and pH_o dependence of acid extrusion (H^+ sensitivity is asymmetric across membrane). *A*, external H^+ sensitivity. Hill plots of acid efflux *versus* pH_o determined at various values of pH_i (pH_i: 6·65, ○; 6·75, ■; 6·85, △; 6·95, ▲). Data from Fig. 9. J_e and J_{max} are the net acid efflux and the maximum acid efflux at a given pH_o and at various values of pH_i. Hill slopes (coefficients) are respectively 1·16, 1·10, 1·30 and 1·20 (least-squares linear regression). A single line (for convenience) is fitted (least squares) to all the points (slope = 1·14). Inset shows Dixon plot of efflux^{-1} (mequiv l^{-1} min^{-1})$^{-1}$

intuitively. It indicates that the apparent affinity of Na^+–H^+ exchange for *extracellular* H^+ ions is decreased in response to a fall of pH_i. This complements the previous observation that a fall of pH_o decreases the apparent affinity of Na^+–H^+ exchange for *intracellular* H^+ ions (Fig. 8).

The influence of pH_i upon pK_o evident in Fig. 9 has been plotted in Fig. 10. Reducing pH_i from 6·95 to 6·65 (0·3 pH units) decreases pK_o by a similar amount (pK_o decreases from 7·42 to 7·08; 0·34 pH units). In a total of five experiments, we found that the mean slope of the relationship (as shown in Fig. 10) was $1·46 \pm 0·36$. Thus the influence upon pK_o of changing pH_i is probably larger than the corresponding influence upon pK_i of changing pH_o (the leftward shift of the activation curves shown in Fig. 8 is suggestive of a much lower slope; at a maximum it would be 0·3–0·4).

In other cell types, elevating pH_o in the range from 6·0 to 8·0 stimulates acid efflux, but raising pH_o above 8·0 then *inhibits* it (e.g. Aronson, 1985). The reason for the decrease in efflux at high pH_o in other tissues is unclear and is possibly unrelated to the more usual stimulatory effect of alkaline pH_o (see Aronson, 1985). In our work such inhibition at high pH_o (8·50) was not typically observed.

Comparison between external and internal pH dependence

Figure 11*A* shows Hill plots constructed for the pH_o sensitivity of acid efflux recorded at the four values of pH_i shown in Fig. 9. The plots are reasonably parallel with a slope (Hill coefficient) varying between 1·1 and 1·3, i.e. the slope appears to be independent of pH_o. In five fibres, the mean Hill coefficient for $[H^+]_o$ inhibition was $1·23 \pm 0·04$. This indicates that inhibition is proportional to $[H^+]^n_o$ where n, on average, equals 1·2, suggesting that one (but possibly > 1) H^+ ion binds to an external site in order to promote inhibition. Further evidence for H_o^+ interaction at a single site in the Purkinje fibre is the observation that a Dixon plot of reciprocal efflux rate *vs.* $[H^+]_o$ is linear, as shown in the inset to Fig. 11*A*, indicating that inhibition of acid efflux appears to be a hyperbolic function of the extracellular H^+ ion concentration. This would be in agreement with the stoichiometry of $[H^+]_o$ inhibition deduced for Na^+–H^+ exchange in renal vesicles (Aronson, Suhm & Nee, 1983), lymphocytes (Grinstein, Cohen & Rothstein, 1984) and cultured osteoblasts (Green, Yamaguchi, Kleeman & Muallem, 1988).

In contrast, the pH_i dependence for stimulation of acid extrusion appears to be a steeper function than the pH_o dependence for inhibition. This is illustrated in Fig. 11*B* which shows a plot of log efflux *versus* log $[H^+]_i$ at various values of pH_o (data extracted from Fig. 8). It should be emphasized that these are *not* Hill plots. The maximum extrusion rate ($V_{max,i}$) at low pH_i was not available so that we were unable to plot the data according to the Hill convention. Instead we measured the maximum slope of the double-logarithmic plots in Fig. 11*B* since this should provide at least an empirical estimate of the steepness of dependence of acid extrusion upon $[H^+]_i$. The slope of the four plots is close to 2·0. In four fibres, the mean slope was $2·02 \pm 0·15$ ($n = 17$) indicating that in the pH_i range from 7·2 to 6·8, acid extrusion is proportional to $[H^+]_i^n$ where $n = 2·0$. This steep dependence of extrusion upon

versus $[H^+]_o$, determined at constant pH_i of 6·85. Data again from Fig. 9. *B*, internal H^+ sensitivity. Plots of log acid efflux *versus* pH_i determined at various pH_o (pH_o; 8·5, ○; 8·0, ●; 7·5, ▲; 7·0, △; data from an experiment similar to those in Figs 2 and 6). Maximal slope of all four plots is similar. Mean slope = 2·1.

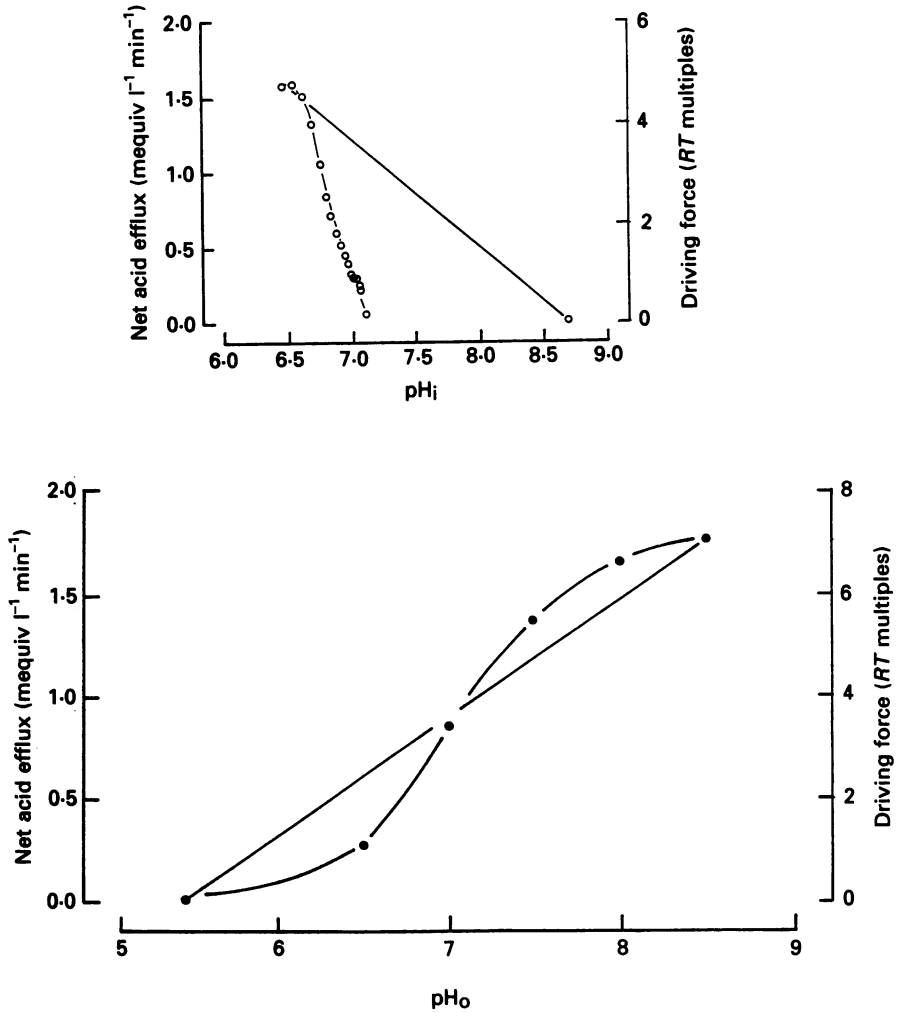

Fig. 12. Inhibition of acid efflux by reduced pH_o does not correlate linearly with the concomitant decline in chemical driving force. ● denotes experimental data taken from Fig. 9 (constant pH_i of 6·65), refer to left-hand ordinate. The straight line shows the calculated decline in driving force. Driving force is expressed (right-hand ordinate) as multiples of RT using the equation:

$$\text{SA3 driving force} = 2{\cdot}3RT\left(\log_{10}\frac{Na_o^+}{Na_i^+} + pH_o - pH_i\right)$$

where $Na_o^+ = 148$ mM, $Na_i^+ = 9{\cdot}6$ mM, $pH_i = 6{\cdot}65$ and R and T have their usual meanings. Inset shows acid efflux (left-hand ordinate, ○) and driving force (right-hand ordinate, straight line) plotted *versus* intracellular pH. Experimental data taken from Fig. 8 for the case where pH_o was 7·5. Driving force calculated using equation above.

intracellular $[H^+]$ is similar to that derived for Na^+–H^+ exchange in skeletal muscle (Vigne, Frelin & Lazdunski, 1982) and cardiac myocytes (Frelin, Vigne & Lazdunski, 1985) and a little higher than that seen in renal vesicles and brain synaptosomes (Aronson, 1985; Jean *et al.* 1985; $n \sim 1{\cdot}4$). The important point is that an exponent

of 2·0 is significantly higher than the average exponent of 1·2 seen here for H^+ inhibition at the external site. We conclude, therefore, that the pH sensitivity of Na^+–H^+ exchange in the Purkinje fibre is asymmetric with respect to H^+ ion binding at the internal and external face and that, over the non–saturating pH range (6·5–7·5), exchange activity is more sensitive to changes of pH_i than pH_o.

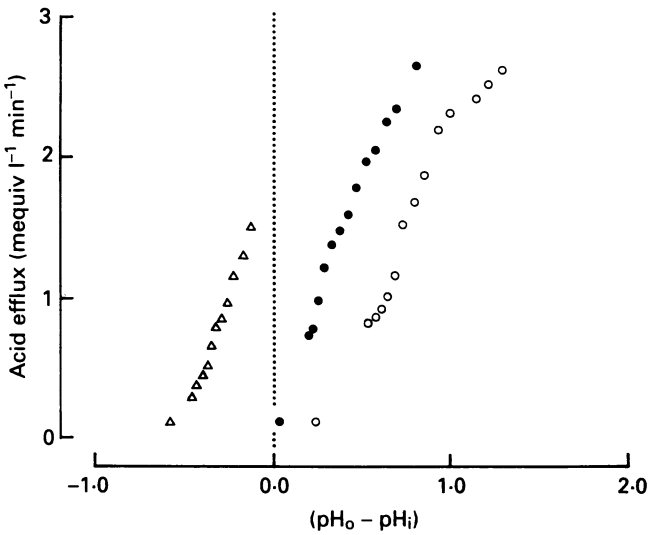

Fig. 13. Acid efflux can still occur when the chemical gradient for H^+ ions is reversed from an outward to an inward gradient (in all cases *total* chemical driving force (cf. legend to Fig. 12) is outward). Acid efflux is plotted *versus* ($pH_o - pH_i$) for case where pH_o is 8·0, ○; 7·4, ●; 6·5, △. Vertical dotted line intersects abscissa at zero H^+ gradient.

Tests of hypotheses for H_o^+ inactivation of Na^+–H^+ exchange

In this section, we investigate two possible mechanisms for H_o^+ inactivation: (i) it is simply related to the decrease in chemical driving force for acid extrusion and (ii) it is due to the removal of the ($pH_o - pH_i$) difference (recall that, at rest, pH_i is usually less than pH_o). Put another way, owing to its sensitivity to pH_o and pH_i, acid extrusion may be set principally by the magnitude of the transmembrane H^+ ratio.

H_o^+ inhibition does not increase linearly with decreased driving force

Firstly, it is well documented that for Na^+–H^+ exchange, the decrease in acid efflux as intracellular pH is raised is not linearly related to the decreased chemical driving force (Aronson, 1985), and cardiac cells are no exception here. The decrease in efflux with elevated pH_i is shown in the inset to Fig. 12; superimposed upon this is the corresponding linear decline in chemical driving force (see legend for details). As pH_i increases, acid efflux declines much more steeply than the driving force. The main part of Fig. 12 now shows that the same observation applies for H_o^+ inhibition. Here the measured decrease in acid efflux with decreasing pH_o is compared with the driving force. Unlike driving force, which decreases linearly with pH_o, efflux declines sigmoidally and, over the pH_o range from 8·0 to 6·5, efflux declines 2–3 times more

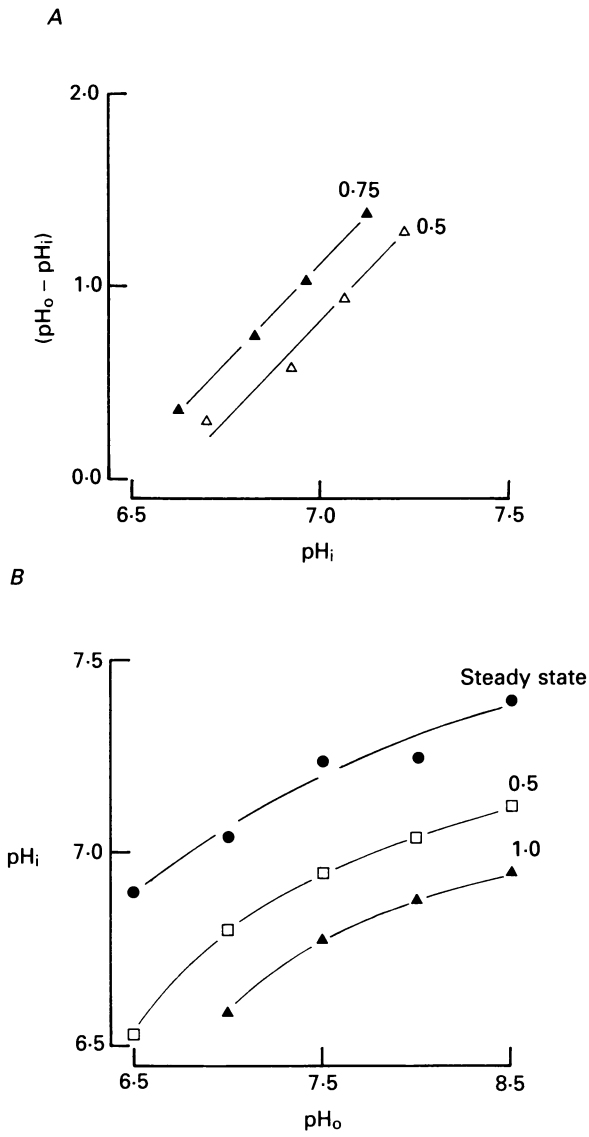

Fig. 14. *A*, acid efflux is not a unique function of H^+ ion gradient ($pH_o - pH_i$). Graph shows value of ($pH_o - pH_i$) that must be imposed in order to maintain a *constant* acid efflux (0·75 mequiv l^{-1} min^{-1}, ▲; 0·5 mequiv l^{-1} min^{-1}, △) when pH_i is varied by ~ 0·75 units. *B*, slope of pH_i *versus* pH_o relationship is the same for various constant values of acid efflux (1·0 mequiv l^{-1} min^{-1}, ▲; 0·5 mequiv l^{-1} min^{-1}, □; 0·1 mequiv l^{-1} min^{-1}, ●; this last plot represents pH_i *vs.* pH_o in the steady state). See text for details.

steeply than driving force. Exchanger activity in response to changing pH_o is therefore not a simple, linear function of driving force. Other, kinetic constraints must be influencing the mechanism.

Acid efflux can occur when pH_o is less than pH_i

One possible kinetic constraint is that an outwardly directed H^+ gradient may be an absolute requirement for acid efflux i.e. $[H^+]_i > [H^+]_o$ (Green *et al.* 1988). In Fig. 13, using data from an experiment similar to that shown in Figs 2 and 6, we have plotted acid efflux *versus* the transmembrane H^+ gradient ($pH_o - pH_i$) for three pH_i recoveries recorded at pH_o 6·5, 7·4 and 8·0. When ($pH_o - pH_i$) on the abscissa is a positive term, the H^+ gradient is outwardly directed and when negative it is inward. In all three cases, *irrespective* of whether ($pH_o - pH_i$) is positive or negative, acid efflux increases steeply with the increasing ($pH_o - pH_i$) gradient and it increases with a similar slope. This shows that acid extrusion can proceed easily, even in the face of an inwardly directed H^+ gradient.

Constant ($pH_o - pH_i$) does not produce constant acid efflux

Given a sufficiently large Na gradient, it is possible that the transmembrane H^+ *ratio* determines acid extrusion (cf. Jean *et al.* 1985). If this were true, then efflux would be related uniquely to ($pH_o - pH_i$). This is not the case as shown in Fig. 14*A*. Here, using data from Fig. 8, we estimate the ($pH_o - pH_i$) difference that must be imposed in order to maintain a *constant* acid efflux when pH_i is raised from 6·6 to 7·2. It is clear that, at an appropriate pH_i, a constant acid efflux can be produced even though the ($pH_o - pH_i$) difference is varied fourfold. Thus the transmembrane H^+ ratio *per se* cannot be setting exchange activity.

The two plots shown in Fig. 14*A* are reasonably parallel. This phenomenon is illustrated in a different way in Fig. 14*B* where values of pH_i required to maintain a constant acid efflux following changes of pH_o have been plotted. Two constant values of efflux have been selected (see legend). Also plotted are the values of pH_o and pH_i observed *in the steady state*. In all three plots, the relationships form shallow curves which are parallel. This suggests that, in the steady state, the pH_i *versus* pH_o relationship is determined directly by the pH_i and pH_o-dependent properties of Na^+–H^+ exchange.

DISCUSSION

In cardiac tissue, as in other tissues, intracellular H^+ ions stimulate Na^+–H^+ exchange whereas extracellular H^+ ions inhibit it. We are principally concerned here with the inhibitory effect. When considering its mechanism we shall, first of all, list the ways in which inhibition is *not* occurring. Although many mechanisms of H_o^+ inhibition can be postulated some are clearly inconsistent with the present data. Four current possibilities for inhibition can now be dismissed.

(1) Inhibition of pH_i recovery at low pH_o is not due to an increase in passive H^+ influx (through pathways other than Na^+–H^+ exchange). In the steady state, background acid loading is independent of pH_o and is reduced by manoeuvres that inhibit glycolysis, indicating that it is primarily a *de novo* generation of metabolic

acid, such as lactic acid (cf. Bountra *et al.* 1988 and Allen *et al.* 1987 for other descriptions of background acid loading in heart caused by glycolysis). In CO_2–HCO_3^--buffered media, however (which were deliberately avoided in the present work), background acid loading may not necessarily remain independent of pH_o since Cl^-–HCO_3^- exchange and a possible HCO_3^- ion conductance will offer appreciable pathways for a pH_o-sensitive H^+-equivalent influx. The pH_o independence of background acid loading in HEPES-buffered media has the interesting consequence that, in the steady state, acid extrusion via Na^+–H^+ exchange (which must balance acid loading) will also be independent of pH_o. We return to this point later.

(2) Inhibition of Na^+–H^+ exchange at low pH_o is not related simply to the reduction in the thermodynamic driving force. The present work shows that acid efflux depends upon pH_i and pH_o in a highly non-linear fashion. This, coupled with the asymmetry in pH dependence at the internal and external face, points to a complex kinetic behaviour of the exchanger with respect to H^+ ions.

(3) Inhibition at low pH_o is not due to removal or even reversal of the transmembrane H^+ gradient. In most cell types, pH_i at rest is less than pH_o, and so the chemical H^+ gradient is outwardly directed. It is often suggested that this fact may be of physiological significance. Jean *et al.* (1985) propose that, in brain synaptosomes, the transmembrane H^+ ratio (i.e. $pH_o - pH_i$) is the important determinant of acid extrusion and Green *et al.* (1988) extend this proposal by suggesting that, in osteoblasts, the exchanger can extrude acid only if the H^+ gradient is outwardly directed. Both of the above proposals do not apply to Na^+–H^+ exchange in the cardiac Purkinje fibre and given the general similarity of the exchanger in the three preparations, it seems likely that the proposals do *not* apply in the other cell types either. Quite obviously, Na^+–H^+ exchange must respond to both pH_i *and* pH_o. Nevertheless, it is the *absolute* value of these parameters that is important for setting extrusion rate and not simply their numerical difference. As an illustration, Fig. 14*A* shows that the transmembrane H^+ ratio can, at appropriate values of pH_i and pH_o, be varied fourfold for no change in extrusion rate. Furthermore, we find that acid extrusion can proceed even when the chemical H^+ gradient has been reversed, i.e. $pH_i > pH_o$ (providing of course, that sufficient energy is available in the Na^+ gradient to drive acid extrusion). Thus it would appear that, at least as far as Na^+–H^+ exchange is concerned, the normally outwardly directed H^+ gradient in the steady state does not have any special physiological significance.

(4) Inhibition at low pH_o does not occur via a significant reduction in the slope of the efflux *versus* pH_i relationship as occurs, for example, for H_o^+ inhibition of acid extrusion in the giant barnacle muscle fibre (Boron, McCormick & Roos, 1979). Our data (Fig. 11*B*) suggest that, at low pH_o, the number of intracellular H^+ ions binding per exchanger unit remains the same, although the apparent intracellular H^+ affinity is reduced.

Exchange activity is set by both pH_i and pH_o

We find that, in cardiac tissue, the dependence of acid extrusion upon pH_i is modulated by pH_o and vice versa. These transmembrane effects of pH are manifested as changes in the apparent external and internal affinities for H^+ ions (pK_o and pK_i). Hence a reduction of pH_o reduces pK_i while a reduction of pH_i reduces pK_o. The

importance of this phenomenon is best appreciated by referring to Fig. 15. In Fig. 15*A*, the dependencies of Na^+–H^+ exchange upon pH_i and pH_o have been superimposed graphically by using a common pH axis to define both internal and external pH. This format emphasizes that activation by $[H^+]_i$ and inactivation by $[H^+]_o$ occurs over a common pH range, with a significant region of cross-over between pH 6·5 and 8·0. At rest, the internal site is represented as being about 10% activated by H_i^+ ions whereas the external site will be about 60% inactivated by H_o^+ ions. In Fig. 15*B*, we see the effect of reducing pH_i (to 6·6) at constant pH_o (7·4). The steep pH_i curve ensures a high activation following intracellular acidosis but sensitivity to *extracellular* pH is also altered. There is an increase in $V_{max,o}$ and decrease in pK_o of the pH_o curve. Consequently, even though pH_o has not changed, the exchanger will now be only about 20% inactivated by H_o^+ ions, i.e. reducing pH_i appears to remove some of the external H^+ inactivation thus reinforcing stimulation of the exchanger. Figure 15*C* shows that the opposite happens if pH_o is reduced (to 6·4) at constant pH_i (7·2). As expected, external H^+ inactivation increases but there is also a leftward shift in the pH_i curve and consequently a decrease of activation by internal H^+ ions.

Is pK_i really reduced by low pH_o? Although we attribute the leftward shift of the pH_i curve (Fig. 15*C*) to a fall in pK_i, our data cannot provide conclusive proof of this without information regarding $V_{max,i}$ (maximal rate at low pH_i). If $V_{max,i}$ were unaffected by pH_o, then the leftward shift seen in Fig. 8 upon moving from pH_o 8·0 to 7·0 would indicate a fall in pK_i of 0·3–0·4 pH units. If $V_{max,i}$ were *also*, reduced, the fall in pK_i would be $< 0·3$.

We would point out that the two previous reports of a decrease in pK_i with pH_o (Jean *et al.* 1985; Green *et al.* 1988) are also troubled by the same problem discussed here. In both papers the authors present no firm evidence concerning possible simultaneous changes in $V_{max,i}$. Thus the apparent shift in pK_i has not strictly been proven yet in *any* preparation, although the data are strongly suggestive of a shift occurring.

When considering the opposite effect (i.e. the decrease in apparent pK_o following a decrease of pH_i) then our own data would seem to be conclusive, since we can measure changes in both pK_o *and* $V_{max,o}$. Thus the transmembrane effect of pH_i upon apparent H_o^+ affinity seems clear whereas the effect of pH_o upon H_o^+ affinity is strongly indicated by the data but not fully proven. What *is* clear, however, is that reducing pH_o shifts the visible portion of the pH_i curve to the left (Fig. 15*C*) thus inhibiting acid efflux.

The rather complex H_i^+ and H_o^+ sensitivity of the exchanger in the Purkinje fibre is similar to that reported in brain synaptosomes (Jean *et al.* 1985) and cultured osteoblasts (Green *et al.* 1988) although there is an important quantitative difference. In these other preparations the leftward shift of the pH_i curve (in pH units) during external acidosis (Fig. 15*C*) was roughly equal to the decrease in pH_o whereas, in the Purkinje fibre, the shift is only about one-third of the pH_o change. This has important consequences in cardiac tissue. If no other acid transport is operating, then pH_i *in the steady state* will be changed by one-third of the change in pH_o. This is precisely what is observed experimentally in cardiac tissue (Fig. 14*B*; also cf. Deitmer & Ellis, 1980; Weissberg *et al.* 1989), the relationship between pH_i and pH_o in the steady state is roughly linear, with a slope of $\sim 0·3$. This occurs because a decrease in pH_o of, say, 1·0 pH units does not change the steady-state background loading rate, whereas, because of the leftward shift in the pH_i curve ($\sim 0·3$ pH units), it inhibits Na^+–H^+ exchange. Hence pH_i will fall. A new steady state will be achieved when the control level of acid extrusion has been re-established, at the expense of

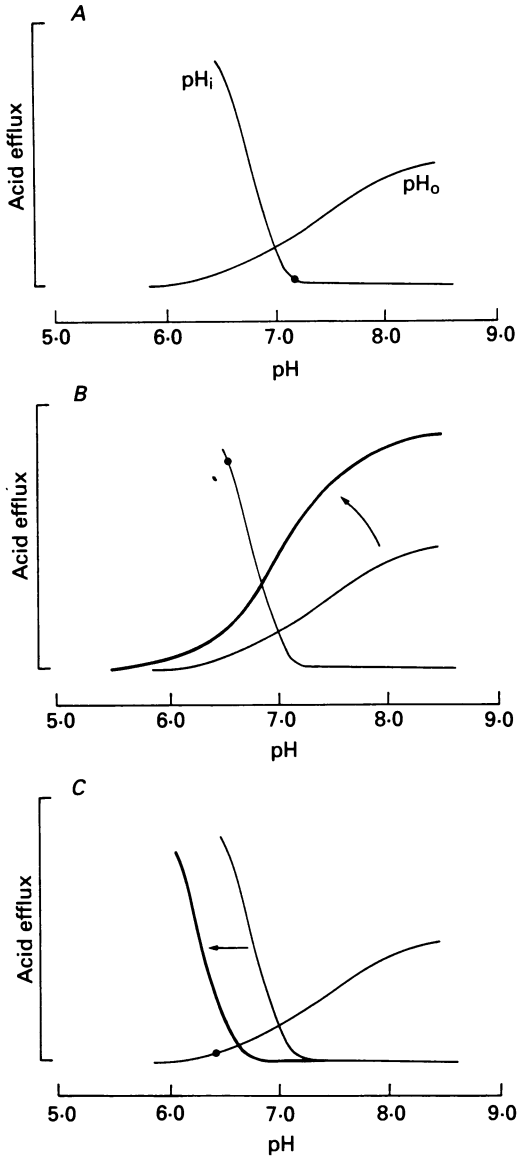

Fig. 15. Diagrammatic summary of response of Na^+–H^+ exchange to a change in pH_i and pH_o. Abscissa refers to pH_i (the graph with negative slope) *or* pH_o (positive slope graph). *A*, resting condition. pH_i is 7·20 (● on pH_i graph) while pH_o is 7·40 (not indicated on graph). *B*, effect of intracellular acidosis. pH_i reduced to 6·70 (● on pH_i graph) while pH_o remains at 7·40. Acid efflux is strongly activated at the internal site as shown, but the pH_o curve has now changed (see thickened curve), $V_{max,o}$ is elevated and pK_o has decreased. Thus external H_o^+ inactivation has been reduced in response to intracellular acidosis. *C*, effect of extracellular acidosis. pH_o reduced from 7·40 to 6·40 (● on pH_o graph) while pH_i remains at 7·20. Acid efflux is strongly inhibited at the external site as shown, but the pH_i curve has now changed (see thickened curve), shifting in parallel to the left. Thus internal H^+ activation has been reduced in response to extracellular acidosis.

allowing pH_i to fall by 0·3 pH units. The influence of pH_o upon pH_i in the steady state is thus a reflection of the H_o^+ inactivation of Na^+–H^+ exchange.

The larger leftward shifts of the pH_i curves seen during external acidosis in brain synaptosomes and osteoblasts might imply a much steeper pH_i *vs.* pH_o relationship in the steady state, with a slope of $\sim$ 1·0. No information is available regarding steady-state pH_i in these preparations but a slope of unity would be somewhat surprising since most other cell types display a slope similar to that of the cardiac Purkinje fibre (e.g. Thomas, 1974; Aickin & Thomas, 1977; Aickin, 1984; Tolkovsky & Richards, 1987; Weissberg *et al.* 1989). In future, it will be of interest to see if the H_o^+ sensitivity of Na^+–H^+ exchange in a variety of other tissues resembles that seen in the present work. For example, data presented recently by Tolkovsky & Richards (1987) for Na^+–H^+ exchange in superior cervical ganglion cells suggest a similar H_o^+ sensitivity. Reducing pH_o by 1·0 pH unit decreases pH_i by 0·2 pH units but does not affect the $t_{0.5}$ for pH_i recovery, very similar to our observations in the Purkinje fibre. It seems possible, therefore, that the H_o^+ sensitivity of Na^+–H^+ exchange described here may be common to all cells where the exchanger exists, although there may be variations in the quantitative details.

Candidates remaining for H_o^+ inhibition

There is, as yet, no universal scheme for Na^+–H^+ transport but simultaneous kinetic mechanisms (as opposed to ping-pong mechanisms) have been favoured (Aronson, 1985; Green *et al.* 1988; Montrose & Murer, 1988). In fact, it is not established firmly that H^+ ions are counter-transported with Na^+ rather than OH^- ions being co-transported with Na^+. Nevertheless H^+ and not OH^- movement is usually assumed and, in line with this consensus, we attribute our low pH_o inhibition to H_o^+ inactivation rather than OH_o^- activation. An obvious model would be one where raising $[H^+]_o$ promotes H_o^+–Na_i^+ exchange thus producing a unidirectional H^+ influx which, with further reductions of pH_o, would increasingly short-circuit H^+ efflux; at equilibrium unidirectional H^+ influx and efflux would be identical. In this case, the pH_o inhibition of acid efflux would actually represent the pH_o activation of unidirectional acid influx through the exchanger, i.e. H^+ influx would be maximal at low pH_o and 50% activated in the pH_o range 7·0–7·4 (pK_o). H^+-dependent shifts in pK_i and pK_o, however, cannot be predicted intuitively from such a model without defining whether the kinetic scheme is simultaneous or ping-pong and whether the H_o^+ inhibition is competitive or non/uncompetitive. A model where Na_o^+ and H_o^+ compete for attachment at the same external carrier site has been postulated previously (Aronson *et al.* 1983). The Hill coefficient for H_o^+ inhibition reported in the present work (1·23) is fairly close to 1·0 so that H_o^+ binding may be occurring at a single site. We have also found (Vaughan-Jones & Wu, 1989) that external H^+ ions inhibit the ability of Na_o^+ ions to activate the exchanger and that this effect is partly competitive. Nevertheless, competition with Na_o^+ accounts for only a lesser fraction of the inhibition by H_o^+ ions (about 20%; Vaughan-Jones & Wu, 1989). A simple reversible, competitive model therefore seems inadequate to explain H_o^+ inhibition in the Purkinje fibre. Indeed we cannot say, at present, whether the externally bound H^+ ion is transported into the cell or whether it merely occupies its receptor and inhibits the acid efflux mode. In this respect, the transmembrane effects of pH

reported here could be due to an allosteric modulation by H^+ ions of the exchanger's transport sites rather than being a natural kinetic consequence of the transport scheme (cf. Montrose & Murer, 1988). Given the complexity, however, inherent in allosteric trans-modulation, we would incline to the latter explanation (i.e. a product of the kinetic scheme), although the kinetic mechanism itself must remain undefined.

Physiological relevance of H_o^+ inactivation

The pH dependence of Na^+–H^+ exchange is important physiologically because changes in both pH_o and pH_i are common occurrences in the heart. Bountra & Vaughan-Jones (1989) have shown recently that intracellular acidosis can actually *increase* contractility because of stimulation of Na^+–H^+ exchange which increases Na^+ influx and thus secondarily elevates $[Ca^{2+}]_i$ via Na^+–Ca^{2+} exchange. If extracellular pH is also reduced, the increase in contractility is abolished since low pH_o inhibits Na^+–H^+ exchange. The sensitivity of the exchange to pH_o thus defines whether an intracellular acidosis will stimulate or depress contraction. It is notable that depression of contraction is most profound in myocardial ischaemia, a condition associated with a fall of both pH_i *and* pH_o and a condition now known to be associated with inactivation of Na^+–H^+ exchange (cf. de Hemptinne & Vanheel, 1988). Part of this inactivation is likely to be caused by the fall in pH_o.

The sensitivity of steady-state pH_i to pH_o also seems to be an important consequence of Na^+–H^+ exchange activity. The carrier's H_o^+ dependence is such that any major extracellular pH change will be transmitted to the cytoplasm in an attenuated form (about 30% of the pH_o change). Thus the exchanger acts as an important membrane defence mechanism against extracellular pH changes. The present work was carried out in HEPES-buffered media and so the extent to which the above mechanism dominates pH_i–pH_o interactions in CO_2–HCO_3-buffered media remains to be assessed; however, it is notable that the slope relating pH_i to pH_o in CO_2–buffered HCO_3 media retains a value of 0·3–0·4 (Ellis & Thomas, 1976).

Finally the pK_o for H_o^+ inhibition of acid extrusion is 7·0–7·4 (depending upon pH_i). Thus, under physiological conditions, the exchanger is up to 50% inactivated at its external site. It is thus ideally poised to respond to both a rise and fall of extracellular pH by respectively increasing and decreasing its rate. Extracellular pH will thus be an important modulator of acid extrusion in the heart.

Supported by funding from the British Heart Foundation (R.D.V.-J.) and National Science Council, Republic of China (Taiwan). We thank Dr Keith Buckler for commenting upon an earlier version of the manuscript, Mr Barry Martin and Mrs Ankaret Wimshurst for technical assistance and Rixons Ltd for their kind co-operation in providing the biological material.

REFERENCES

AICKIN, C. C. (1984). Direct measurement of intracellular pH and buffering power in smooth muscle cells of guinea-pig vas deferens. *Journal of Physiology* **349**, 571–585.

AICKIN, C. C. & THOMAS, R. C. (1977). Micro-electrode measurement of the intracellular pH and buffering power of mouse soleus muscle fibres. *Journal of Physiology* **267**, 791–810.

ALLEN, D. G., MORRIS, P. G., ORCHARD, C. H. & PIROLO, J. S. (1985). A nuclear magnetic resonance study of metabolism in the ferret heart during hypoxia and inhibition of glycolysis. *Journal of Physiology* **361**, 185–204.

ARONSON, P. S. (1985). Kinetic properties of the plasma membrane Na^+–H^+ exchanger. *Annual Review of Physiology* **47**, 545–560.

ARONSON, P. S., SUHM, M. A. & NEE, J. (1983). Interaction of external H^+ with the Na^+–H^+ exchanger in renal microvillus membrane vesicles. *Journal of Biological Chemistry* **258**, 6767–6771.

BORON, W. F., MCCORMICK, W. C. & ROOS, A. (1979). pH Regulation in barnacle muscle fibres: dependence on intracellular and extracellular pH. *American Journal of Physiology* **237**, C185–193.

BOUNTRA, C., KAILA, K. & VAUGHAN-JONES, R. D. (1988). Mechanism of rate-dependent pH changes in the sheep cardiac Purkinje fibre. *Journal of Physiology* **406**, 483–501.

BOUNTRA, C., POWELL, T. P. & VAUGHAN-JONES, R. D. (1990). Comparison of intracellular pH transients in single ventricular myocytes and isolated ventricular muscle of guinea-pig. *Journal of Physiology* **424**, 343–365.

BOUNTRA, C. & VAUGHAN-JONES, R. D. (1989). Effect of intracellular and extracellular pH on contraction in isolated, mammalian cardiac muscle. *Journal of Physiology* **418**, 163–187.

DE HEMPTINNE, A. & VANHEEL, B. (1988). Intracellular pH and Na^+ activity during simulated ischaemia in isolated guinea-pig ventricular muscle. *Journal of Physiology* **407**, 115*P*.

DEITMER, J. W. & ELLIS, D. (1980). Interactions between the regulation of the intracellular pH and sodium activity of sheep cardiac Purkinje fibres. *Journal of Physiology* **304**, 471–488.

ELLIS, D. (1977). The effects of external cations and ouabain on the intracellular sodium activity of sheep heart Purkinje fibres. *Journal of Physiology* **273**, 211–240.

ELLIS, D. & THOMAS, R. C. (1976). Microelectrode measurement of the intracellular pH of mammalian heart cells. *Nature* **262**, 224–225.

FRELIN, C., VIGNE, P. & LAZDUNSKI, M. (1985). The role of the Na^+/H^+ exchange system in the regulation of the internal pH in cultured cardiac cells. *European Journal of Biochemistry* **149**, 1–4.

GREEN, R. D., FRELIN, C., VIGNE, P. & LAZDUNSKI, M. (1986). The activity of the Na^+/H^+ antiporter in cultured cardiac cells is dependent on the culture conditions used. *FEBS Letters* **196**, 163–166.

GREEN, J., YAMAGUCHI, D. T., KLEEMAN, C. R. & MUALLEM, S. (1988). Cytosolic pH regulation in osteoblasts. Interaction of Na^+ and H^+ with the extracellular and intracellular faces of the Na^+/H^+ exchanger. *Journal of General Physiology* **92**, 239–261.

GRINSTEIN, S., COHEN, S. & ROTHSTEIN, A. (1984). Cytoplasmic pH regulation in thymic lymphocytes by an amiloride-sensitive Na^+/H^+ antiport. *Journal of General Physiology* **83**, 341–369.

JEAN, T., FRELIN, C., VIGNE, P., BARBRY, P. & LAZDUNSKI, M. (1985). Biochemical properties of the Na^+/H^+ exchange system in rat brain synaptosomes. *Journal of Biological Chemistry* **260**, 9678–9684.

KAILA, K. & VAUGHAN-JONES, R. D. (1987). Influence of sodium–hydrogen exchange on intracellular pH, sodium and tension in sheep cardiac Purkinje fibres. *Journal of Physiology* **390**, 93–118.

MONTROSE, M. H. & MURER, H. (1988). Kinetics of Na^+/H^+ exchange. In *Na^+/H^+ Exchange*, ed. GRINSTEIN, S., pp. 57–75. CRC Press Inc., Boca Raton, FL, USA.

PIWNICA-WORMS, D., JACOB, R., HORRES, R. C. & LIEBERMAN, M. (1985). Na/H exchange in cultured chick heart cells – pH_i regulation. *Journal of General Physiology* **85**, 43–64.

ROOS, A. & BORON, W. F. (1981). Intracellular pH. *Physiological Reviews* **61**, 296–434.

THOMAS, R. C. (1974). Intracellular pH of snail neurones measured with a new pH-sensitive glass micro-electrode. *Journal of Physiology* **238**, 159–180.

TOLKOVSKY, A. M. & RICHARDS, C. D. (1987). Na^+/H^+ exchange is the major mechanism of pH regulation in cultured sympathetic neurons: measurements in single cell bodies and neurites using a fluorescent pH indicator. *Neuroscience* **22**, 1093–1102.

VANHEEL, B., DE HEMPTINNE, A. & LEUSEN, I. (1986). Influence of surface pH on intracellular pH regulation in cardiac and skeletal muscle. *American Journal of Physiology* **250**, C748–760.

VAUGHAN-JONES, R. D. (1988*a*). Regulation of intracellular pH in cardiac muscle. In *Proton Passage Across Cell Membranes*, Ciba Foundation Symposium 139, pp. 23–46. Wiley, Chichester.

VAUGHAN-JONES, R. D. (1988*b*). pH-selective microelectrodes: construction and use in investigation of transmembrane sodium/hydrogen exchange. In *Na^+/H^+ Exchange*, ed. GRINSTEIN, S., pp. 3–19. CRC Press Inc., Boca Raton, FL, USA.

VAUGHAN-JONES, R. D. & WU, M.-L. (1989). Mechanism of inhibition of Na–H exchange by external protons in the isolated sheep cardiac Purkinje fibre. *Journal of Physiology* **417**, 55*P*.

VAUGHAN-JONES, R. D., WU, M.-L. & BOUNTRA, C. (1989). Sodium–hydrogen exchange and its role in controlling contractility during acidosis in cardiac muscle. *Molecular and Cellular Biochemistry* **89**, 157–162.

VAUGHAN-JONES, R. D. & WU, M.-L. (1990). pH dependence of intrinsic H^+ buffering power in the sheep cardiac Purkinje fibre. *Journal of Physiology* **425**, 429–448.

VIGNE, P., FRELIN, C. & LAZDUNSKI, M. (1982). The amiloride-sensitive Na^+/H^+ exchange system in skeletal muscle cells in culture. *Journal of Biological Chemistry* **257**, 9394–9400.

WEISSBERG, P. L., LITTLE, P. J., CRAGOE, E. J. JR & BOBIK, A. (1989). The pH of spontaneously beating cultured rat heart cells is regulated by an ATP–calmodulin-dependent Na^+/H^+ antiport. *Circulation Research* **64**, 676–685.

WU, M.-L. & VAUGHAN-JONES, R. D. (1988). Inhibition of Na–H exchange in the sheep cardiac Purkinje fibre. *Journal of Molecular and Cellular Cardiology* **20**, suppl. IV, S47.